Journal of African Earth Sciences 243 (2026) 106292

Contents lists available at ScienceDirect

Journal of African Earth Sciences

journal homepage: www.elsevier.com/locate/jafrearsci

Groundwater depletion under climate and human pressures: MODFLOW modeling and prospective scenarios for central Tunisia

Kaouther Ncibi[a,b], Younes Hamed[a,b], Yosra Ayadi[a,b], Riheb Hadji[c], Mabrouk Mosbahi[d,e,f,*], Malika Abbes[g], Matteo Gentilucci[h], Tullio Tucciarelli[d]

[a] University of Gafsa, Faculty of Sciences of Gafsa, Laboratory for the Application of Materials to the Environment, Water and Energy (LAMEEE), City Campus Sidi Ahmed Zarroug, Gafsa, 2112, Tunisia
[b] International Association of Water Resources in the Southern Mediterranean Basin, Gafsa, 2112, Tunisia
[c] Laboratory of Applied Research in Engineering Geology, Geotechnics, Water Sciences, and Environment, Setif 1 University, Setif, 19000, Algeria
[d] University of Palermo, Department of Engineering, 90128, Italy
[e] Higher Institute of Applied Sciences and Technology of Gafsa, University of Gafsa, Gafsa, 2112, Tunisia
[f] Laboratory of Electro-Mechanic Systems (LASEM), National School of Engineers of Sfax (ENIS), University of Sfax, B.P. 1173, km 3.5 Soukra, Sfax, 3038, Tunisia
[g] Institute of Hydro-Meteorological of Training and Research of Oran, P.O. Box 7019, Seddikia, Oran, 31025, Algeria
[h] School of Science and Technology, Geology Division, University of Camerino, Camerino, 62032, Italy

ARTICLE INFO

Handling Editor: Zakaria Hamimi

Keywords:
Groundwater modeling
MODFLOW
Sidi Bouzid
Central Tunisia
Prospective scenarios
Sustainable management

ABSTRACT

Groundwater resources in arid and semi-arid regions face mounting pressure from population growth and agricultural intensification. In central Tunisia, the Sidi Bouzid North (SBN) basin relies critically on its shallow aquifer system to meet water demands. This study develops a numerical groundwater flow model using MODFLOW, calibrated over a 29-year period (1990-2019), to assess the current state of the aquifer and simulate its future evolution. Steady-state and transient calibrations yielded correlation coefficients of 0.97 and 0.95, respectively, confirming the model's reliability. The 2019 water balance reveals a structural deficit of 17.24 Mm^3/year, reflecting increasing overexploitation since 1990. Two prospective scenarios were developed for 2050: a climate scenario incorporating an 18% rainfall reduction based on national climate projections, and an anthropogenic scenario combining reduced recharge with a continuation of the current exploitation trend. The climate scenario produces a modest average piezometric decline of 0.3 m, whereas the anthropogenic scenario results in a far more severe drop of 1.8 m, six times greater, underscoring that human pressure is the dominant driver of aquifer degradation. Peripheral basin areas are identified as the most vulnerable to drying. These findings call for urgent action, including withdrawal reduction, artificial recharge, and enhanced piezometric monitoring, to ensure sustainable groundwater management in this water-stressed region.

1. Introduction

Groundwater is one of the world's most precious and heavily used natural resources, particularly in arid and semi-arid regions where surface water resources are limited, unpredictable, and subject to significant climate variability (Hamed et al., 2024a, 2024b). In recent decades, rapid population growth and the intensification of agricultural practices have led to a considerable increase in groundwater extraction, generating growing pressure on often fragile and vulnerable aquifer systems. Unlike surface water, groundwater has a particularly slow renewal cycle and a low natural recharge capacity, making it highly susceptible to overexploitation and human-induced disturbance (Sherwood Lollar et al., 2024; Saccò et al., 2024). This reality underscores the urgent need for better understanding, monitoring, and management of these strategic resources to ensure their sustainability for future generations (Hamed et al., 2018; Hajji et al., 2021; Ayadi et al., 2025).

In this context, central Tunisia, and more specifically the Sidi Bouzid region, perfectly illustrates the pressures on groundwater resources in semi-arid Mediterranean zones (Ncibi et al., 2021; Missaoui et al., 2023). Characterized by an arid-to-semi-arid climate, low and irregular annual rainfall, and a predominantly agricultural economy, this region is heavily dependent on groundwater for irrigation, drinking water supply, and socio-economic development (Ncibi et al., 2021, 2023; Hamed et al., 2022). For several decades, the aquifers of the Sidi

* Corresponding author. University of Palermo, Department of Engineering, 90128, Italy.
E-mail address: mabrouk.mosbahi@unipa.it (M. Mosbahi).

https://doi.org/10.1016/j.jafrearsci.2026.106292
Received 14 April 2026; Received in revised form 17 July 2026; Accepted 17 July 2026
Available online 18 July 2026

Bouzid North basin have been subjected to intensive exploitation, resulting in a progressive decline in piezometric levels, a reduction in exploitable reserves, and, in some areas, qualitative degradation of groundwater (Jellalia et al., 2015; Hamdi et al., 2020). These trends are consistent with those reported in other semi-arid Mediterranean basins, where groundwater overexploitation has been identified as a major threat to long-term water security (Lachaal et al., 2012; Trabelsi et al., 2013; Bougghariou et al., 2018).

It is clearly from this perspective that hydrogeological modeling reveals its full relevance as an investigative and decision-making tool (Ben Saad et al., 2023; Cid-Escobar et al., 2024). Generally speaking, hydrogeological modeling involves a simplified representation of natural complexity and the unattainable reality (Vats et al., 2020; Toscani et al., 2022). It relies on a set of assumptions and simplifications aimed at reproducing, acceptably, the behavior of a complex natural system. In this sense, a model can be considered "the result of a compromise between generality, realism, and accuracy" (Kauark-Leite and Nascimento, 1993), seeking to reconcile the need to faithfully represent physical processes with the constraints related to data availability and computing power. Far from being an exact reproduction of reality, the model constitutes a conceptual and numerical tool allowing us to test hypotheses, interpret observations, and simulate prospective scenarios under controlled conditions (Bougghariou et al., 2018; Leone et al., 2024).

Among the numerical modeling tools for groundwater flow, the MODFLOW code, developed by the United States Geological Survey (USGS), has become the most widely used and proven international standard for simulating flow in saturated porous media (Langevin et al., 2017; Zeydalinejad, 2022). Based on the finite difference method and the three-dimensional solution of the hydraulic diffusivity equation, MODFLOW allows for the simulation of groundwater flow in steady-state and transient regimes, takes into account interactions between groundwater and surface water, and integrates various boundary conditions and source terms representing pumping, recharge, and drainage (Vellando et al., 2020; Singh and Pathania, 2025). Its robustness, flexibility, and widespread use within the scientific community make it a particularly suitable tool for studying different types of aquifer systems, such as those in the SBN basin.

In Tunisia, several MODFLOW-based studies have been conducted to assess groundwater dynamics in various basins. Lachaal et al. (2012) applied MODFLOW to the Zéramdine-Béni Hassen Miocene aquifer system and highlighted progressive piezometric decline linked to agricultural overexploitation. Trabelsi et al. (2013) demonstrated, through numerical modeling of the Nabeul-Hammamet basin, that combined climatic and anthropogenic effects accelerate piezometric degradation in areas with high borehole density. More recently, Gharbi et al. (2023) developed a conceptual and numerical hydrogeological model of the shallow aquifer of Sidi Bouzid North, providing a retrospective analysis of overexploitation impacts over the period 1989–2015. However, these studies share important limitations: they focus primarily on historical reconstruction without developing quantified prospective simulations, they do not explicitly separate the relative contributions of climate change and human overexploitation to aquifer degradation, and they provide limited spatially explicit guidance for prioritizing management interventions at the basin scale.

These research gaps highlight the need for a modeling study that goes beyond retrospective analysis to provide quantified, scenario-based projections of aquifer evolution, while explicitly distinguishing the respective roles of climatic and anthropogenic drivers. In the Sidi Bouzid North basin, no study to date has developed prospective simulations to assess the future trajectory of the aquifer under contrasting climate and exploitation scenarios, nor has any work provided spatially explicit identification of the most vulnerable zones to guide targeted management interventions. The present study addresses these gaps by developing and applying a calibrated MODFLOW model over 29 years (1990-2019), and by simulating two contrasting scenarios to 2050: a climate scenario incorporating projected rainfall reduction, and an anthropogenic scenario reflecting the continuation of current exploitation trends. This approach enables, for the first time in this basin, a quantified comparison of the relative impacts of climate change and human pressure on groundwater depletion, providing actionable spatial guidance for sustainable aquifer management.

The specific objectives of this study are: (i) to develop and calibrate a numerical MODFLOW groundwater flow model for the Sidi Bouzid North aquifer system using a comprehensive 29-year database; (ii) to establish the water balance for the reference year 2019 and assess the current state of overexploitation; (iii) to simulate the future evolution of piezometric levels under climate and anthropogenic scenarios to 2050; and (iv) to identify the most vulnerable zones and formulate concrete recommendations for sustainable and integrated groundwater management in the basin.

2. Materials and methods

2.1. Study area

2.1.1. Geography and climate

The study area of the Sidi Bouzid North (SBN) basin covers 1508 km^2 in central Tunisia, North Africa (Fig. 1). It is characterized by an elevation ranging between 238 m and 640 m above sea level. The minimum and maximum average temperatures are observed in January and July with values equal to 5.9°C and 33.16°C, respectively. As for the annual average temperature, it is equal to 19.71°C for the period 1990-2020. The values of the average monthly evapotranspiration are variable during the year in the study area, with minimum values recorded in February equal to 20.7 mm and maximum values of the order of 180 mm in July (Ncibi et al., 2020a, 2020b2021, 2023; Missaoui et al., 2022).

2.1.2. Hydrology

Two main wadis characterize the SBN basin, which are Oued El Fekka and Oued El Hjal (Fig. 1). El Fekka Wadi, originating in Algeria, crosses the alluvial aquifer of the southern part of the study area. It ends its course in the evaporation depression of Neggada and gives birth to Oued Neggada, which extends downstream by Oued El Hjal. Finally, Oued El Hjal, before reaching the Sidi Saad dam, receives from its left part the Oueds of Sbitla and Jilma. The confluence of Oueds El Htob and El Hjal thus forms the outline of Oued Zéroud, where the Sidi-Saâd dam is located (Ncibi et al., 2020a, 2020b).

2.1.3. Geology and hydrogeology

The study area is represented in asymmetrical synclinal basins formed during the Mio-Plio-Quaternary detrital deposits. These synclinal basins are the result of the compressive phase, which affected the entire areas of central Tunisia at the beginning of the Miocene, resulting in the genesis of the Atlas folds whose substratum is formed by the Cretaceous and Miocene deposits (Chaabane et al., 2024). The oldest deposits are attributed to the Triassic and Jurassic outcropping on raised structures bordering the study area (Ncibi, 2022). The collapsed areas of the Sidi Bouzid North basin are covered by Tertiary (Paleogene, Neogene, and Miocene) and Quaternary (fluvial and aeolian deposits, mainly detrital with high permeability) deposits (Fig. 1).

The SBN basin aquifer system is located within a Mio-Plio-Quaternary (MPQ) formation and constitutes a regionally extensive unconfined phreatic aquifer (Aydi et al., 2013; Jmal et al., 2022). This formation is characterized by predominantly sandy-gravelly detrital deposits, indicating relatively high permeability and good transmissivity of the aquifer, favorable to the circulation and storage of groundwater (Fig. 2). These hydrodynamic characteristics give this aquifer significant water potential, but also vulnerability to intensive withdrawals and climatic variations.

The groundwater monitoring network in the Sidi Bouzid North basin consists of observation wells and piezometers distributed across the

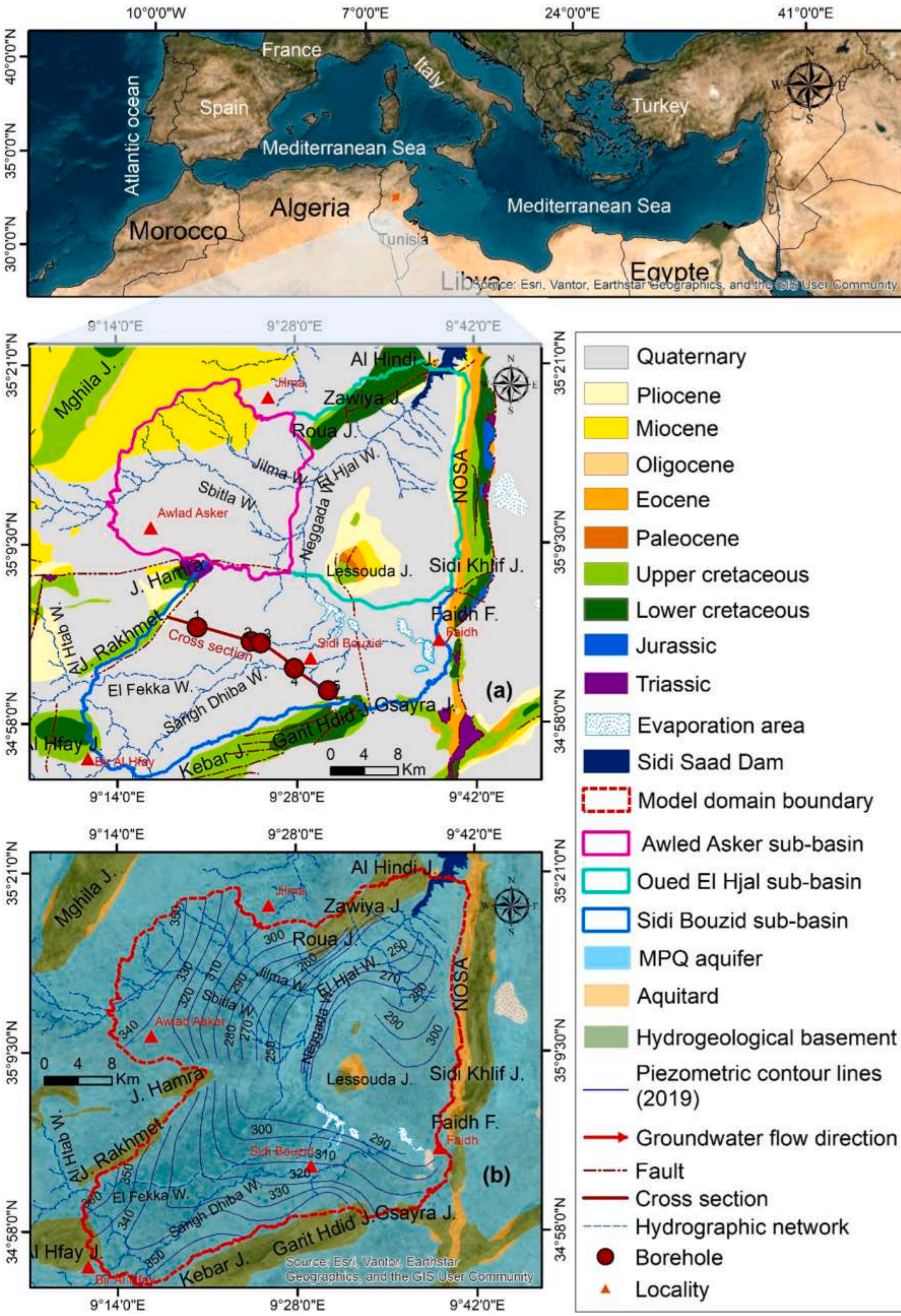

Fig. 1. Location of the study area (the Sidi Bouzid North basin, central Tunisia): **(a)** geological map; **(b)** hydrogeological map.

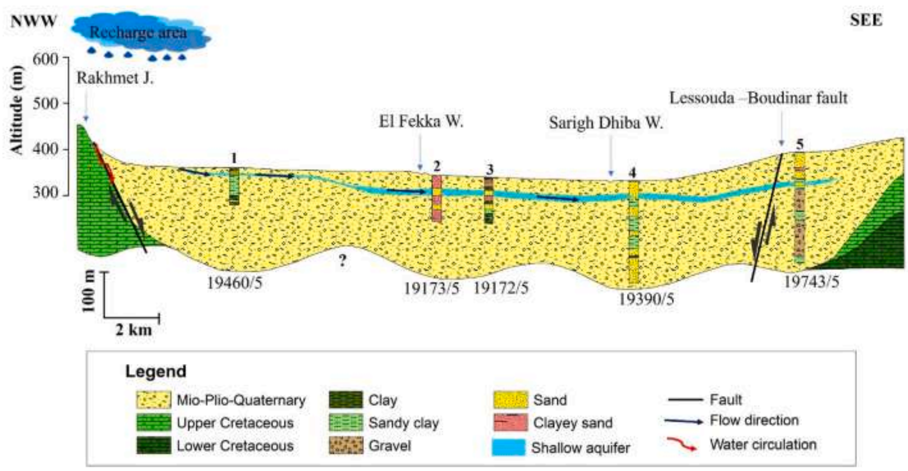

Fig. 2. Lithostratigraphic cross-section of the study area.

basin to ensure representative spatial coverage of the aquifer system (Fig. 1). Groundwater level (GWL) data were collected periodically by the DGRE and CRDA over a 29-year observation period spanning from 1990 to 2019. A total of 43 observation wells were used for steady-state calibration (1990), while 53 observation wells were used for transient calibration over the period 1991–2019. The recorded groundwater levels range from approximately 290 m in the northern and eastern parts of the basin to 360 m in the southern and western zones, reflecting the general southwest-to-northeast flow gradient (Ncibi, 2022). Groundwater depth (GWD) varies spatially from 25 m in the northern sector to 45 m in the southwestern part of the basin, with a basin-wide average of approximately 35 m (Ncibi, 2022). The time series of piezometric measurements is characterized by a semi-annual measurement frequency, providing a consistent and sufficiently dense temporal record to capture both seasonal fluctuations and long-term trends in groundwater levels.

2.2. Groundwater modeling

2.2.1. Data processing

The construction and calibration of the numerical groundwater flow model for the SBN basin are based on a multidisciplinary and multisource database covering a 29-year observation period, from 1990 to 2019. Piezometric data were collected from the General Directorate of

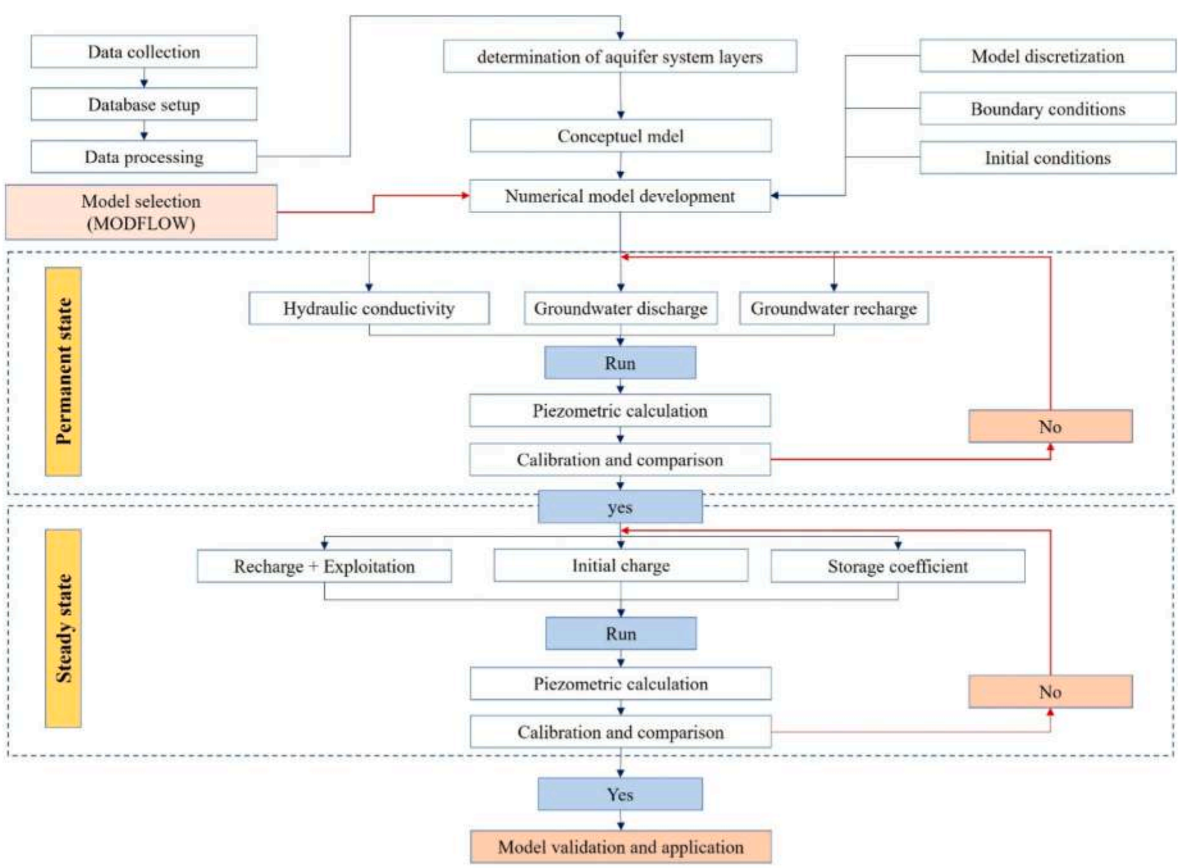

Fig. 3. Flowchart showing the numerical groundwater flow modelling procedure.

Water Resources (DGRE, 2020) and the Regional Commission for Agricultural Development (CRDA, 2020) of Sidi Bouzid governorate, from a network of 43 observation wells used for steady-state calibration (1990) and 53 observation wells used for transient calibration over the period 1991–2019. Climate data, including monthly rainfall, temperatures, and potential evapotranspiration (PET), were provided by the National Institute of Meteorology (NIM) and were used to estimate groundwater recharge and characterize seasonal and interannual variations in water inputs into the aquifer system. Operational data, relating to pumping rates and the number of active pumping wells in the basin, were also obtained from the CRDA (2020) and the DGRE (2020).

2.2.2. Model construction

The construction of the numerical model of groundwater flow in the SBN basin was carried out using the Visual MODFLOW software, based on data preparation (Fig. 3). Three-dimensional groundwater flow can be mathematically represented given the following equation based on water mass balance and Darcy's law equations, Eq. (1) (McDonald and Harbaugh, 1988; Langevin et al., 2017; Zeydalinejad, 2022):

$$\frac{\partial}{\partial x}\left[K_x\frac{\partial h}{\partial x}\right]+\frac{\partial}{\partial y}\left[K_y\frac{\partial h}{\partial y}\right]+\frac{\partial}{\partial z}\left[K_z\frac{\partial h}{\partial z}\right]-w=S_s\frac{\partial h}{\partial t} \quad \text{Eq.1}$$

Where Kx, Ky, and Kz are the hydraulic conductivity values along the x, y, and z coordinate axes, which are assumed to be parallel to the major hydraulic conductivity axes, w is the volumetric flow per unit volume and represents the sources (w is negative) and/or sinks (w is positive) of water per unit time, h is the hydraulic head, Ss is the specific storage of the porous material and t is the time.

The aquifer system was conceptualized using a two-layer model. The first layer represents the unconfined phreatic aquifer, composed of sandy-gravelly Mio-Plio-Quaternary deposits, with a hydraulic conductivity of 2×10^{-4} m/s (DGRE, 2020; Ncibi, 2022). The second layer represents an impermeable to semi-impermeable clayey formation underlying the aquifer, with a hydraulic conductivity of 2×10^{-6} m/s (DGRE, 2020; Ncibi, 2022). This second layer does not constitute an aquifer but serves as a lower confining boundary in the model. Its inclusion is justified by two complementary reasons: (i) it allows the representation of limited downward vertical leakage from the phreatic aquifer towards deeper formations, a process observed in the basin and supported by the lithostratigraphic cross-sections (Fig. 2); and (ii) it contributes to reducing model calibration error by providing a more realistic representation of the lower boundary condition of the aquifer system.

The modelling domain covers a total area of 1508 km^2, discretized into 3600 rectangular cells (60 columns and 60 rows). Cells located outside the aquifer's extent zones were inactivated to accurately represent the actual geometry of the water table. The topography was integrated from a Digital Elevation Model (DEM, 30 m resolution), resampled to the model's grid, while the top and bottom of the groundwater aquifer were interpolated from available well and borehole cross-sections. The bedrock elevation surface defining the bottom of the aquifer was constructed using lithological and stratigraphic data obtained from 25 well logs provided by the DGRE and CRDA. The base of the Mio-Plio-Quaternary aquifer formation, corresponding to the top of the underlying impermeable clayey layer, was identified in each borehole log and georeferenced to its spatial coordinates. These point data were then spatially interpolated across the model domain using the kriging interpolation method available in the Visual MODFLOW environment, producing a continuous bedrock elevation surface at the model grid resolution. The thickness of the first layer, representing the unconfined phreatic aquifer, varies spatially from approximately 60 m in the southern zone to 80 m in the northeastern and northwestern parts of the basin, reflecting the progressive thickening of the Mio-Plio-Quaternary deposits towards the center and periphery of the basin in accordance with the regional geological structure. The second layer, representing the underlying semi-impermeable clayey formation, was assigned a uniform thickness of 20 m throughout the model domain, consistent with its role as a lower confining boundary rather than an active flow unit.

Two types of boundary conditions were used to define the hydrodynamic behavior of the system. The Dirichlet condition (type 1), corresponding to a head-constrained boundary, is represented by the lateral boundaries of the basin: mountain ranges are considered head-constrained boundaries, while lateral connections with neighbouring aquifers are represented by 34 cells with non-zero head. The Neumann condition (type 2) represents the recharge and discharge zones of the aquifer, incorporating rainwater recharge, runoff from the El Fekka, Sarigh Dhiba, Sbitla, and Jilma wadis as head-constrained drains, the contribution of the Sidi Saad dam represented by 3 cells, as well as the discharge zones downstream of Oued El Hjal and the Neggada evaporation zone, represented by 33 cells with head-constrained drains (Fig. 4). Groundwater recharge is primarily ensured by the direct infiltration of rainwater, estimated according to DGRE indices at 6% of rainfall in areas of high permeability at the level of wadi beds, and at 4% in the rest of the study area with moderate permeability (Castany, 1968, 1982). Reinfiltration of irrigation water in irrigated areas was estimated at 1.5% of the volumes extracted. Pumping, constituting the main well term in the model, was integrated based on operational data provided by the DGRE (2020) and the CRDA (2020), distributed across all active grid cells of the model (see Fig. 5).

2.2.3. Model performance evaluation criteria

The performance of the numerical groundwater flow model was evaluated using two complementary quantitative criteria widely adopted in groundwater modeling studies (Moriasi et al., 2007; Anderson et al., 2015).

The first criterion is the Pearson correlation coefficient (R^2), which measures the linear agreement between observed and simulated hydraulic heads across all monitoring points. R^2 ranges from 0 to 1, with values closer to 1 indicating a stronger agreement between simulated and observed values (Moriasi et al., 2007). It is calculated as follows (Eq. (2)):

$$R^2=\left(\frac{\sum_{i=1}^{n}\left(h_{obs,i}-\overline{h}_{obs}\right)\left(h_{sim,i}-\overline{h}_{sim}\right)}{\sqrt{\sum_{i=1}^{n}\left(h_{obs,i}-\overline{h}_{obs}\right)^2\cdot\sum_{i=1}^{n}\left(h_{sim,i}-\overline{h}_{sim}\right)^2}}\right)^2 \quad \text{Eq.2}$$

where $h_{obs,i}$ and $h_{sim,i}$ are the observed and simulated hydraulic heads at monitoring point i, $\overline{h}_{obs}$ and $\overline{h}_{sim}$ are their respective means, and n is the total number of monitoring points.

The second criterion is the Normalized Root Mean Square Error (NRMSE), which measures the average magnitude of the error between observed and simulated hydraulic heads, normalized by the range of observed values to allow comparison across different study areas. It is calculated as follows (Eq. (3)):

$$NRMSE=\frac{\sqrt{\frac{1}{n}\sum_{i=1}^{n}\left(h_{obs,i}-h_{sim,i}\right)^2}}{h_{obs,max}-h_{obs,min}}*100 \quad \text{Eq.3}$$

where $h_{obs,max}$ and $h_{obs,min}$ are the maximum and minimum observed hydraulic heads, respectively. NRMSE is expressed as a percentage, with lower values indicating better model performance (Jafari et al., 2021). Following Anderson et al. (2015), an NRMSE below 10% is generally considered acceptable for groundwater flow models. Both criteria were applied to evaluate model performance under steady-state conditions (reference year 1990) and transient conditions (1991–2019), at all monitoring points distributed throughout the basin.

2.2.4. Model calibration and validation

The calibration and validation of the numerical model were carried

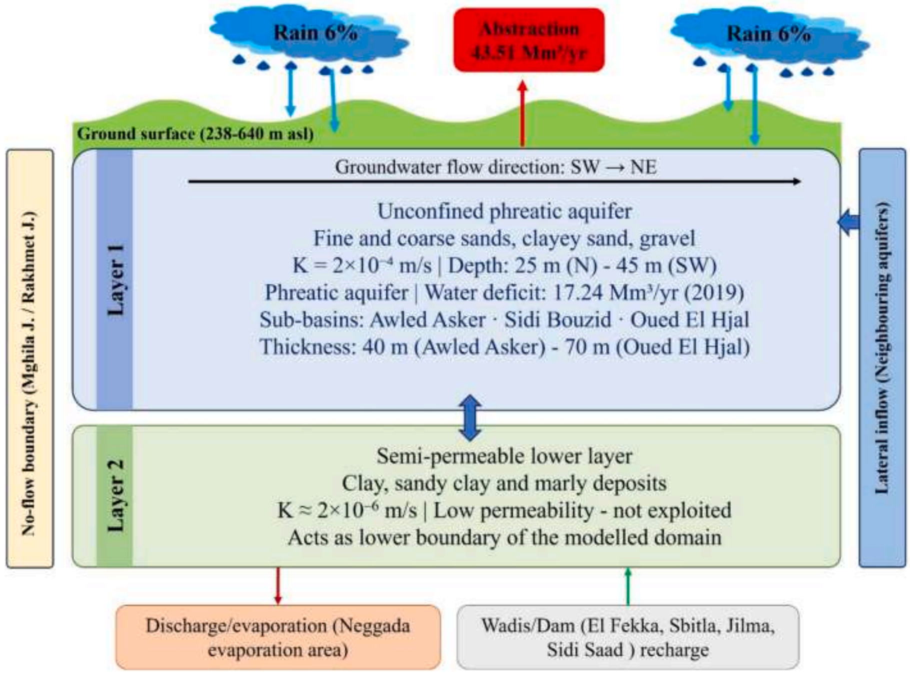

Fig. 4. Conceptual model of the Sidi Bouzid North basin.

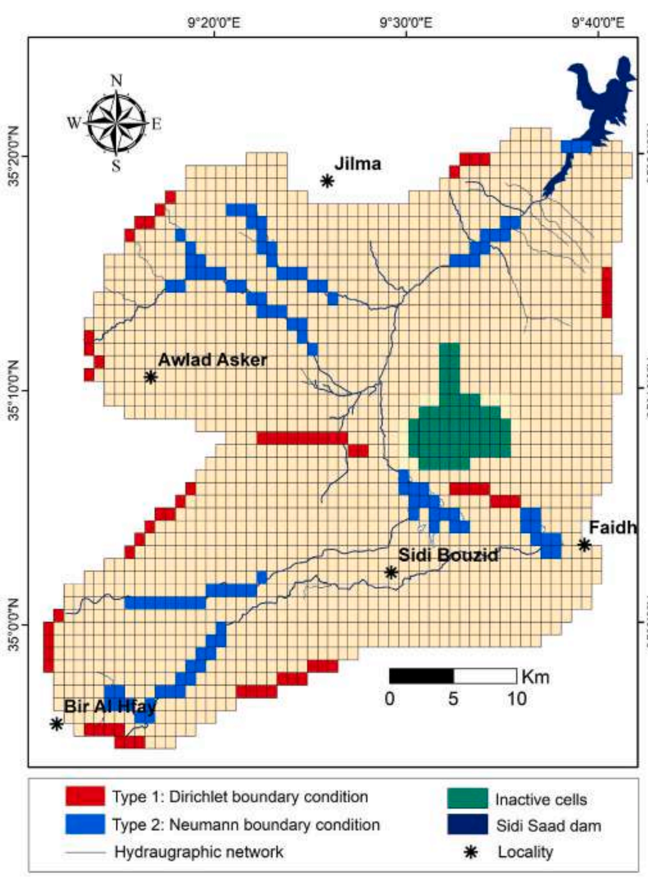

Fig. 5. Boundary conditions of the phreatic aquifer system model of the Sidi Bouzid North basin.

out in two successive and complementary stages, following standard groundwater modeling procedures (Jafari et al., 2021). Steady-state calibration was performed using 1990 as the reference year, a period during which the aquifer system can be considered in approximate hydrodynamic equilibrium, as evidenced by relatively stable piezometric levels recorded during that period (Liang et al., 2023). Steady-state conditions were simulated using mean annual values of recharge and pumping rates for 1990, as annual time steps are appropriate for steady-state calibration since this approach averages out seasonal fluctuations and focuses on reproducing the long-term equilibrium state of the aquifer (Anderson et al., 2015). The calibration consisted of adjusting, using a trial-and-error method, two key parameters: hydraulic conductivity (K) and recharge rate (R), until satisfactory agreement was achieved between observed and simulated hydraulic heads. Observed hydraulic heads used for calibration were collected directly from field measurements at the 43 observation wells for steady-state and 53 observation wells for transient calibration. These field-measured hydraulic heads constitute the primary calibration targets for both steady-state and transient simulations.

Transient-state calibration was conducted over the period 1991-2019 using annual time steps, consistent with the temporal resolution of the available piezometric, pumping, and recharge data provided by the DGRE and CRDA, which are aggregated on a yearly basis (Fig. 3). This temporal discretization is appropriate for capturing long-term trends in groundwater level decline while remaining consistent with the density and frequency of the available observation dataset. The primary parameter adjusted during transient calibration was the specific yield (Sy), which represents the volume of water released from storage per unit decline in hydraulic head in an unconfined aquifer (Anderson et al., 2015). Specific yield was progressively adjusted alongside recharge conditions until the simulated piezometric time series satisfactorily reproduced the observed interannual fluctuations recorded at the monitoring wells. Pumping rates were kept constant at their reported values as provided by the DGRE and CRDA throughout the entire calibration process, without any adjustment. The model was validated by comparing the simulated piezometric levels with the values measured in the field. The model performance was evaluated using the correlation coefficient (R^2) and the normalized root mean square error (NRMSE), ensuring the model's robustness and reliability before any prospective use (Zeydalinejad, 2022).

2.2.5. Sensitivity analysis

A sensitivity analysis was performed to assess the relative influence of the main model parameters on the simulated piezometric levels. Hydraulic conductivity (K), recharge rate (R), and storage coefficient (Ss) were independently varied by ±10%, ±25%, and ±50% from their calibrated values, while all other parameters were held constant (Jafari et al., 2021; Liang et al., 2023). Recharge was incorporated into the sensitivity analysis due to the uncertainty associated with its indirect estimation from empirical infiltration indices rather than direct observations. Given its fundamental role in controlling groundwater heads and its adjustment during the calibration process, recharge strongly influences model behavior. Sensitivity evaluation is therefore critical for assessing model reliability, quantifying uncertainty in calibration results, and prioritizing parameters for improved field characterization (Anderson et al., 2015). The model response was evaluated using the root-mean-square error (RMSE) between the observed and simulated piezometric levels at all monitoring points.

2.2.6. Future simulation scenarios

To anticipate the future evolution of the SBN groundwater aquifer, two prospective simulation scenarios were developed for the year 2050, taking into account the increasing overexploitation recorded since 1991 and the variability of the water balance linked to rainfall and withdrawals. The first scenario, based on natural constraints, simulates the impact of climate change by incorporating an 18% reduction in rainfall by 2050, based on projections from the Tunisian National Strategy for Adapting Agriculture to Climate Change. This would lead to a proportional decrease in recharge, while extraction is maintained at 2019 levels to assess the evolution of the aquifer within the context of resource protection. The second scenario, with anthropogenic constraints, applies the same recharge conditions as the first scenario, but also incorporates a progressive increase in exploitation according to a linear trend adjusted by the least squares method based on historical exploitation data, thus allowing us to estimate the volumes withdrawn up to 2050 and to assess the impact of continuing the current trend on the piezometric levels of the groundwater aquifer. This linear trend is visually represented in Fig. 6 as a trendline fitted to the historical pumping data over the period 1990-2019 and extrapolated to 2050 using the least squares method.

3. Results

3.1. Model calibration and validation

The steady-state calibration, performed using the reference year 1990, yielded good agreement between observed and calculated piezometric levels, confirmed by a correlation coefficient of 0.97 and a normalized root mean square error (NRMSE) of 1.60%, well below the 10% acceptability threshold recommended by Anderson et al. (2015). The hydraulic conductivity values obtained after calibration vary between 9.6×10^{-5} m/s and 1.4×10^{-3} m/s, reflecting the spatial heterogeneity of the hydrodynamic properties of the groundwater aquifer in the study area. Comparison between the calculated and measured piezometric values at reference points shows no significant difference, confirming the validity of the chosen boundary conditions and initial hydrodynamic parameters.

Table 1 presents the individual performance criteria for each of the 43 observation wells used for steady-state calibration. Of these, 17 wells (40%) achieved an Excellent rating (absolute error <1 m) and 24 wells (56%) a Good rating (absolute error between 1 and 3 m), with only 2 wells (5%) rated as Acceptable and none as Poor, confirming the high spatial consistency of the calibrated model across the basin (Figs. 7 and 8).

The transient calibration, conducted over the period 1991–2019 using 53 observation wells, resulted in an average storage coefficient value of 5.8×10^{-4}, with a correlation coefficient of 0.95 and an NRMSE of 1.55%, confirming the robustness of the model over the entire 29-year reference period (Fig. 8). Among the 53 wells, 26 achieved an Excellent rating, 21 a Good rating, and 6 an Acceptable rating, with no Poor ratings recorded, confirming the high spatial consistency of the transient calibration across the basin (Table 1). The water balance calculated for 2019 reveals a total exploitation of 43 Mm^3, accompanied by a progressive decrease in drainage, which reached 0.23 Mm^3, reflecting the significant impact of the intensification of withdrawals on the aquifer system balance between 1990 and 2019.

Table 2 summarizes the global performance statistics for both calibration periods. Under steady-state conditions, the model achieved a mean error (ME) of −0.166 m, a mean absolute error (MAE) of 1.512 m, and a mean relative error of 0.475%. Under transient conditions, performance remained similarly strong, with a ME of 0.044 m, a MAE of 1.543 m, and a mean relative error of 0.490%. These results confirm that the model reliably reproduces observed hydraulic heads under both calibration regimes, providing a solid basis for prospective simulations.

Sensitivity analysis reveals that the simulated piezometric levels are most sensitive to variations in hydraulic conductivity, with a variation of ±50% resulting in an average change in simulated levels of approximately 2.1 m. The recharge rate is the second most influential parameter, while the storage coefficient has a comparatively moderate influence. This hierarchy confirms that the calibration effort was appropriately focused on hydraulic conductivity and recharge as the primary control parameters of the aquifer system (Fig. 9).

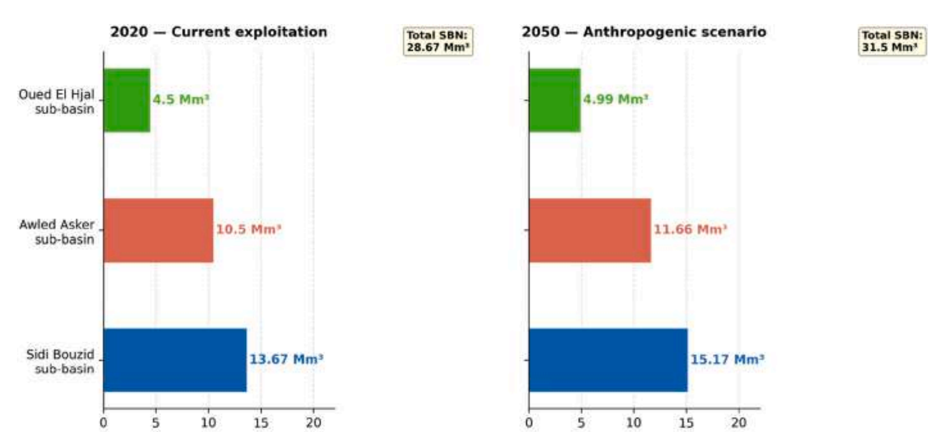

Fig. 6. Groundwater abstraction in 2020 and projected abstraction in 2050 for the three sub-basins of the Sidi Bouzid North basin (Sidi Bouzid sub-basin, Awled Asker, and Oued El Hjal sub-basins).

Table 1
Performance criteria per observation well for steady-state (1990) and transient (1991–2019) model calibration.

Well No.	Steady state			Transient state		
	Abs. Error * (m)	Relative Error * (%)	Performance Evaluation	Abs. Error * (m)	Relative Error * (%)	Performance Evaluation
1	-	-	-	0,262	0,085	Excellent
2	-	-	-	1274	0,395	Good
3	-	-	-	0,413	0,127	Excellent
4	-	-	-	0,265	0,081	Excellent
5	1,25	0,371	Good	3069	0,924	Acceptable
6	2126	0,652	Good	1413	0,432	Good
7	0,882	0,269	Excellent	2233	0,676	Good
8	0,484	0,153	Excellent	0,135	0,044	Excellent
9	0,419	0,126	Excellent	2359	0,726	Good
10	0,161	0,048	Excellent	2989	0,874	Good
11	0,992	0,3	Excellent	0,622	0,187	Excellent
12	1,51	0,44	Good	0,478	0,138	Excellent
13	0,003	0,001	Excellent	0,066	0,019	Excellent
14	0,72	0,224	Excellent	1913	0,598	Good
15	0,145	0,046	Excellent	1084	0,337	Good
16	2665	0,785	Good	1644	0,48	Good
17	1747	0,556	Good	3,43	1118	Acceptable
18	2869	0,829	Good	2577	0,708	Good
19	-	-	-	2084	0,644	Good
20	-	-	-	2,13	0,653	Good
21	-	-	-	1317	0,457	Good
22	2547	0,887	Good	0,857	0,31	Excellent
23	-	-	-	2374	0,86	Good
24	2421	0,814	Good	1863	0,592	Good
25	0,706	0,213	Excellent	1673	0,494	Good
26	1191	0,373	Good	0,289	0,09	Excellent
27	2956	0,979	Good	0,821	0,267	Excellent
28	2505	0,832	Good	2244	0,763	Good
29	-	-	-	0,463	0,153	Excellent
30	1796	0,473	Good	2059	0,567	Good
31	0,137	0,042	Excellent	0,365	0,123	Excellent
32	-	-	-	3447	1148	Acceptable
33	2299	0,833	Good	1447	0,482	Good
34	0,125	0,041	Excellent	1348	0,475	Good
35	1575	0,508	Good	2618	0,891	Good
36	1582	0,498	Good	2015	0,681	Good
37	1557	0,512	Good	0,513	0,175	Excellent
38	2101	0,722	Good	0,813	0,271	Excellent
39	0,634	0,239	Excellent	1281	0,455	Good
40	0,45	0,141	Excellent	1485	0,606	Good
41	0,657	0,212	Excellent	1394	0,423	Good
42	0,328	0,104	Excellent	3594	1229	Acceptable
43	3121	1,04	Acceptable	0,594	0,203	Excellent
44	1,86	0,517	Good	0,203	0,059	Excellent
45	2472	0,899	Good	0,479	0,178	Excellent
46	2858	0,817	Good	2,77	0,815	Good
47	0,966	0,268	Excellent	3959	1129	Acceptable
48	2796	0,799	Good	0,706	0,207	Excellent
49	4402	1295	Acceptable	0,344	0,102	Excellent
50	2347	0,809	Good	1462	0,53	Good
51	1533	0,438	Good	1789	0,49	Good
52	0,058	0,017	Excellent	3274	0,917	Acceptable
53	1,05	0,3	Good	1025	0,29	Good
Performance Evaluation based on Absolute Error rowhead						
Excellent		Good		Acceptable		Poor
Abs. Error < 1 m		Abs. Error 1–3 m		Abs. Error 3–5 m		Abs. Error >5 m

*H_{obs} = Observed hydraulic head (m); H_{sim} = Simulated hydraulic head (m); Residual = $H_{sim} - H_{obs}$; Abs. Error = |Residual|; Relative Error (%). |Res|/Hobs × 100 (Anderson et al., 2015; Moriasi et al., 2007); '-' not included in the corresponding calibration period due to unavailability of observation data.

3.2. Hydrogeological characterization

The groundwater piezometric map established for 2019 shows that the piezometric surface closely follows the general topography of the basin, sloping from the periphery of the hills towards the axes of the El Fekka and El Hjal wadis. The piezometric curves are generally regular and concave downstream, with a variable hydraulic gradient that increases from the edges towards the wadis and from upstream to downstream, reaching its maximum value near the Sidi Saad dam. The general direction of groundwater flow is southwest-northeast, with secondary axes converging towards the El Hjal wadi, which constitutes the main outlet of the aquifer (Fig. 7).

Piezometric analysis reveals three hydrologically distinct sectors. In the southern zone (Sidi Bouzid sub-basin), groundwater levels range from 360 to 290 m. The converging piezometric contours indicate recharge from the Jebel Rakhmet-Hamra and Jebel Kebar highlands. In the western zone (Awled Asker), piezometric levels decrease from 350 m near Jebel Mghila to 250 m close to Oued Neggada, suggesting recharge mainly from the surrounding reliefs. In the eastern zone (Oued El Hjal sub-basin), groundwater levels vary between 300 and 250 m. The wider spacing of the piezometric contours indicates a low hydraulic gradient and groundwater flow towards Oued El Hjal. The groundwater balance,

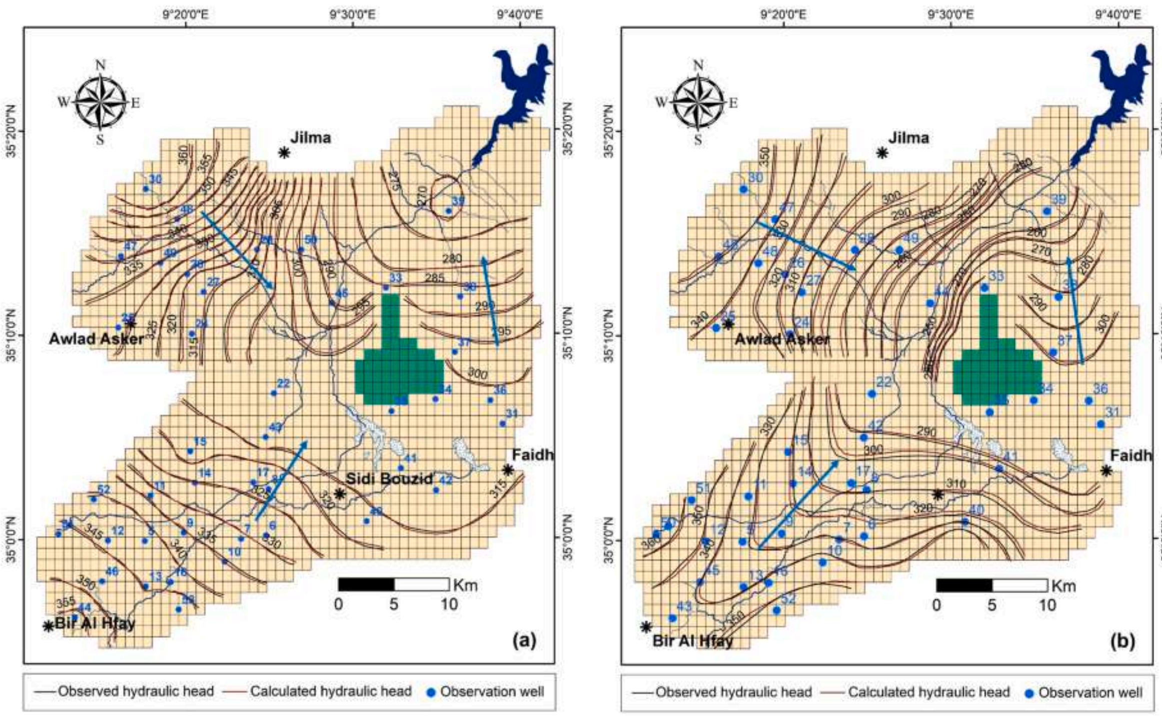

Fig. 7. Simulated and observed piezometric map of the phreatic aquifer of the Sidi Bouzid North basin under: **(a)** steady-state conditions (1990) and **(b)** transient state (2019).

established for the reference year 2019, reveals a pronounced deficit of 17.24 Mm^3/year, indicating a proven overexploitation of the aquifer system, particularly marked in areas with irrigated perimeters (Table 3). The system's inflows are primarily from the infiltration of floodwaters from wadis (16.25 Mm^3/year), rainwater (10.6 Mm^3/year), reinfiltration of irrigation water (1.02 Mm^3/year), and lateral flow from nearby aquifers (0.8 Mm^3/year), for a total inflow of 28.67 Mm^3/year. Outflows are dominated by groundwater extraction, reaching 43.51 Mm^3/year, supplemented by flows to natural outlets (0.7 Mm^3/year), evaporation losses (0.5 Mm^3/year), and flows to nearby aquifers (1.2 Mm^3/year), bringing the total output to 45.91 Mm^3/year. This structural imbalance between inputs and outputs confirms the increasing vulnerability of the groundwater aquifer to intensive exploitation, fully justifying the implementation of prospective simulations and sustainable management scenarios.

3.3. Prospective simulations

Prospective simulations carried out to 2050 using the calibrated MODFLOW model highlight a progressive and differentiated degradation of the piezometric state of the SBN basin's groundwater aquifer according to the two scenarios considered. The first scenario, simulating the impact of climate change through an 18% reduction in rainfall without an increase in water use, reveals an average drop in piezometric levels of 0.3 m by 2050 compared to the 2019 baseline. This is accompanied by the emergence of new dry areas at the foot of Jebel Mghila, Jebel Rakhmet-Hamra, Jebel Al Hfay, and to the east of the study area, indicating localized depletion of the reservoir in the surrounding areas. A local change in flow direction was also observed in the southwest and northeast of the basin, due to a significant piezometric depression. This scenario illustrates the mechanism by which extreme weather events, such as droughts and heavy rainfall, exacerbate water stress: during heavy precipitation, the rapid saturation of the soil surface limits transfer to deeper layers, favoring runoff towards the center of the basin at the expense of recharge in the peripheral areas of the aquifer. The second scenario, incorporating a gradual increase in exploitation according to the current trend, results in a significantly more pronounced average piezometric drop of 1.8 m compared to 2019, with three distinct and particularly vulnerable depression zones: the western zone of the Awled Asker sub-basin with a drop reaching 2.1 m, the western and southwestern zones of the SBN sub-basin with values of 0.9 m, and the eastern zone of the north-south axis at Jebel Sidi Khlif and Jebel Faidh with a decrease of 1.7 m (Fig. 10).

4. Discussion

4.1. Study strengths

The performance metrics obtained during both steady-state and transient calibration confirm the robustness of the developed model. The steady-state calibration achieved a correlation coefficient of $R^2 = 0.97$ and an NRMSE of 1.60%, well below the 10% acceptability threshold recommended by Anderson et al. (2015). The transient calibration over the 29-year period (1991–2019) yielded a correlation coefficient of $R^2 = 0.95$ and an NRMSE of 1.55%, demonstrating the model's capacity to reproduce long-term aquifer dynamics. These metrics are consistent with those reported in comparable MODFLOW-based studies in similar semi-arid contexts (Lachaal et al., 2012; Trabelsi et al., 2013; Izady et al., 2015). The sensitivity analysis further confirmed that hydraulic conductivity and recharge rate are the dominant control parameters of the aquifer system, which is consistent with the hydrogeological characteristics of unconfined aquifers in semi-arid regions (Jafari et al., 2021; Liang et al., 2023), and validates the calibration strategy adopted in this study.

4.2. Climate vs. anthropogenic drivers

Comparing the two scenarios clearly highlights the predominance of anthropogenic pressure over climatic constraints in the degradation of the aquifer's quantitative status, with the second scenario generating a piezometric drop six times greater than the first. Nevertheless, both scenarios converge on the same areas of maximum vulnerability, located

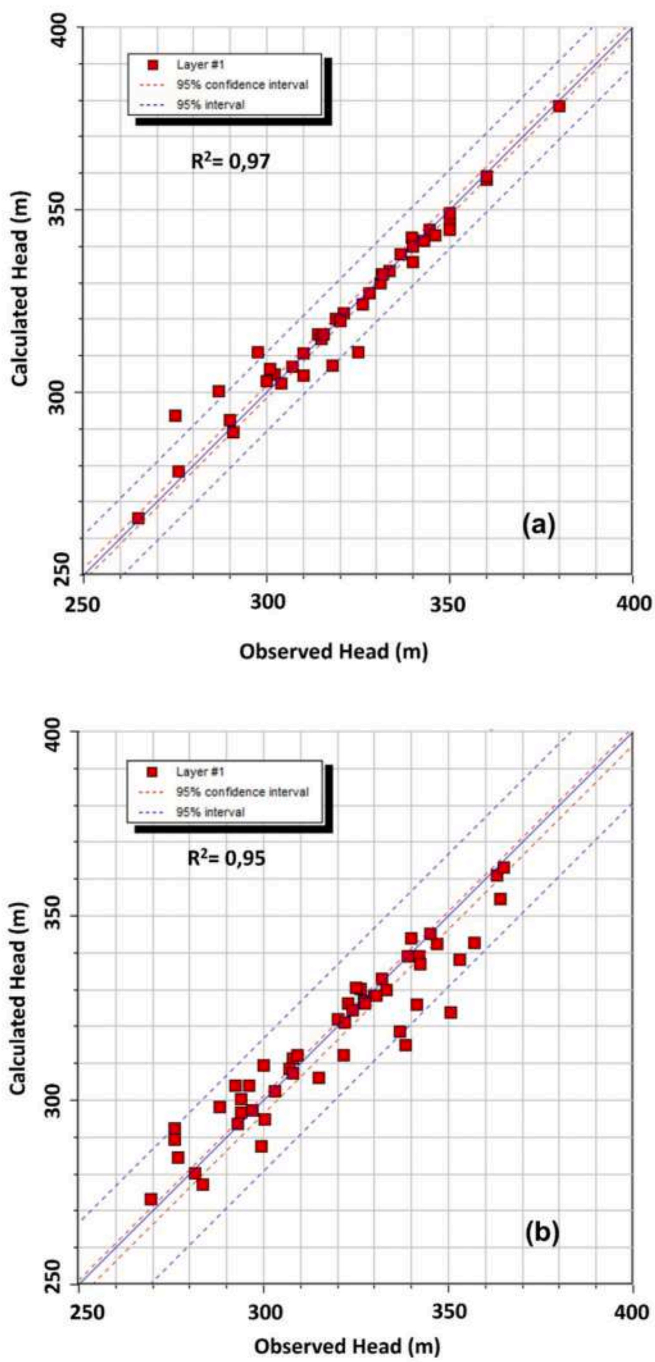

Fig. 8. Scatter plot of observed versus simulated groundwater levels under: **(a)** steady-state conditions and **(b)** transient state conditions.

on the periphery of the basin, whose progressive drying is explained by two concurrent structural factors: (1) the geomorphology of the basin and the geometry of the aquifer, characterized by a thinning of the reservoir in the bordering areas, and (2) the topographic slope, which favors the drainage of groundwater towards the center of the basin at the expense of peripheral areas.

The results of the prospective simulations obtained in this study are consistent with a global trend of groundwater resource degradation observed in many semi-arid basins worldwide (Saccò et al., 2024; Sherwood Lollar et al., 2024), and corroborate the findings of several previous studies conducted in similar hydrogeological contexts (Lachaal et al., 2012; Trabelsi et al., 2013; Boughariou et al., 2018; Izady et al., 2015).

Table 2
Summary of global model performance statistics for steady-state and transient calibration.

Parameters	Steady state	Transient state	Performance
Wells number	43	53	—
ME [a] **(m)**	−0,166	0,044	**≈ 0 ideal**
MAE [a] **(m)**	1512	1543	**< 3 m Good**
RMSE [a] **(m)**	1835	1,86	**< 5 m Acceptable**
NRMSE [a] **(%)**	1596	1,55	**< 10% Acceptable**
Mean Rel. Error (%)	0,475	0,49	**< 2% Good**
R^2	0,97	0,95	**> 0.90 Good**

[a] ME = Mean Error; MAE = Mean Absolute Error; RMSE = Root Mean Square Error; NRMSE = RMSE/(H_max − H_min) × 100; R^2 = Pearson correlation coefficient squared (Anderson et al., 2015; Moriasi et al., 2007).

The average piezometric drop of 0.3 m simulated under the first climate scenario and the 1.8 m drop obtained under the second anthropogenic scenario by 2050 are consistent with trends reported in the hydrogeological literature concerning aquifers in arid and semi-arid Mediterranean regions. In Tunisia, similar results were obtained by Lachaal et al. (2012) in the Zéramdine-Béni Hassen Miocene aquifer system (east-central Tunisia), where MODFLOW modeling highlighted a progressive decline in piezometric levels linked to agricultural overexploitation, with annual deficits comparable to those recorded in the SBN basin. Similarly, Trabelsi et al. (2013) demonstrated through numerical modeling of the Nabeul-Hammamet basin aquifer that the combined effects of climate and anthropogenic activities accelerate piezometric level decline, particularly in areas with high pumping well density. This finding aligns with observations made in the Awled Asker and Oued El Hjal sub-basins. Regarding the drying zones identified on the periphery of the basin, this phenomenon was also reported by Izady et al. (2015) in their MODFLOW modeling study of a semi-arid aquifer in Iran. In this study, the periphery areas consistently exhibited the most pronounced piezometric declines due to reservoir thinning and gravity drainage towards the central areas, a mechanism identical to that observed in the peripheral areas of the SBN basin.

4.3. Limitations and uncertainties

Despite the robustness of the model, several limitations and sources of uncertainty should be acknowledged. First, pumping rates are derived from declared extraction volumes, which may underestimate actual withdrawals in areas with informal or unregistered irrigation wells, a common challenge in agricultural groundwater management in semi-arid regions (Gharbi et al., 2023). Second, the climate scenario is based on a single rainfall reduction projection of 18%, without accounting for the full range of uncertainty associated with regional climate projections. Incorporating multiple climate scenarios from different General Circulation Models (GCMs) would provide a more comprehensive assessment of future aquifer trajectories. These limitations should be addressed in future modeling efforts to further improve the prospective capacity of the model.

4.4. Broader implications for groundwater management

These results call for an urgent review of groundwater management strategies in the SBN basin, including the implementation of measures to reduce withdrawals in the most vulnerable areas, the development of artificial groundwater recharge techniques, and the adoption of a more water-efficient irrigation policy, to preserve the long-term sustainability of this strategic resource in a context of climate change and increasing demand.

At the regional scale, this study makes an original and significant contribution through the development of prospective simulations to 2050 under two distinct scenarios, climatic and anthropogenic, unlike the work of Gharbi et al. (2023), which is limited to a retrospective

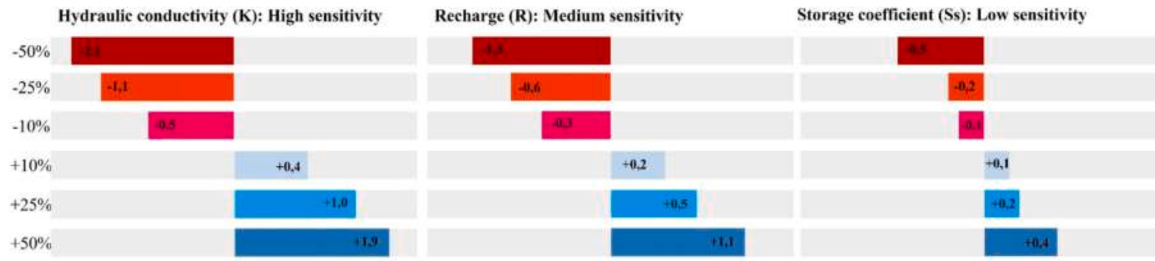

Fig. 9. Sensitivity of simulated piezometric levels to variations in hydraulic conductivity (K), recharge rate (R), and storage coefficient (Ss), expressed as RMSE (m).

Table 3
Water balance of the phreatic aquifer, Sidi Bouzid North basin (2019, Mm^3/yr).

Component	Inflows
Rainfall infiltration	10,6
Wadi flood infiltration	16,25
Irrigation return flow	1,02
Lateral inflow from neighbouring aquifers	0,8
Total inflows	28.67
	Outflows
Groundwater abstraction	43,51
Natural discharge (springs, baseflow)	0,7
Evaporation losses	0,5
Lateral outflow to neighbouring aquifers	1,2
Total outflows	45.91
Water balance	−17,24

analysis of the impacts of overexploitation over the period 1989-2015 without quantified future projections. This prospective approach, absent from previous work conducted on the SBN basin, constitutes an essential decision-making tool for water resource managers, providing them with a quantified and spatially explicit view of the future evolution of the aquifer under different water pressure scenarios. Furthermore, the detailed quantification of the water balance for the reference year 2019, as well as the precise identification of the area's most vulnerable to drying out in the peripheral sectors of the basin, allows for the formulation of concrete and operational management recommendations, going well beyond the simple observation of overexploitation reported by Gharbi et al. (2023).

5. Conclusion

This study demonstrates that numerical groundwater flow modelling, combined with scenario-based prospective simulations, provides a robust and transferable framework for diagnosing aquifer overexploitation and anticipating future groundwater dynamics in semi-arid regions. By explicitly disentangling the respective impacts of climate change and anthropogenic overexploitation, it provides water managers and policymakers with quantitative, spatially explicit information to prioritize interventions where they are most needed. These results enhance our understanding of aquifer system dynamics in semi-arid Mediterranean basins in several crucial respects. Anthropogenic pressure is clearly identified as the primary driver of aquifer degradation, causing a decline six times more severe than that attributable to climate change alone by 2050; this positions demand management and abstraction regulation as priority levers for sustainable groundwater governance. Spatially identifying the most vulnerable peripheral zones provides an operational basis for targeting artificial recharge projects and pumping restrictions at the basin scale. Furthermore, the calibrated

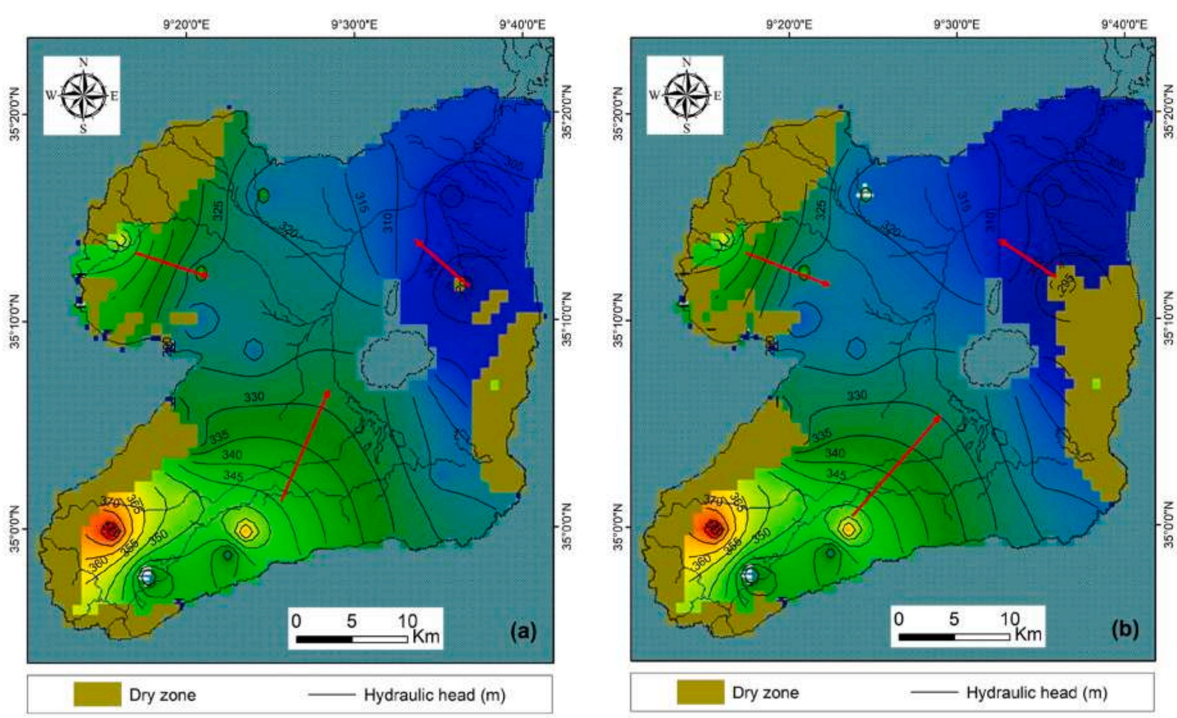

Fig. 10. Simulated piezometric map of the phreatic aquifer of the Sidi Bouzid North basin at the 2050 horizon: **(a)** Scenario 1: climatic constraint and **(b)** Scenario 2: anthropogenic constraint (increasing groundwater abstraction).

MODFLOW model serves as an adaptable decision-support tool, easily modified to evaluate the effectiveness of alternative management strategies as new monitoring data become available. Beyond the Sidi Bouzid North basin, the modeling approach adopted here, combining long-term transient-state calibration, contrasting prospective scenarios, and spatial vulnerability mapping, is directly applicable to other overexploited aquifer systems facing similar challenges across North Africa and the wider Mediterranean region. Future research should prioritize integrating multiple climate scenarios derived from General Circulation Models (GCMs), coupling the flow model with land-use and agricultural demand models, assessing groundwater quality and salinization risks in the most vulnerable areas, and extending the study framework to the basin's deeper confined aquifer systems. Overall, these results confirm that the SBN aquifer is under severe and increasing stress, primarily due to anthropogenic overexploitation; that the developed model is highly reliable ($R^2 = 0.97$ and 0.95; NRMSE $<2\%$); and that targeted demand management in the most vulnerable peripheral areas represents the most urgent and effective pathway toward sustainable groundwater governance in this water-stressed region.

CRediT authorship contribution statement

Kaouther Ncibi: Conceptualization, Data curation, Methodology, Software, Writing – original draft. **Younes Hamed:** Supervision, Validation, Writing – review & editing. **Yosra Ayadi:** Conceptualization, Methodology, Visualization. **Riheb Hadji:** Supervision, Writing – review & editing. **Mabrouk Mosbahi:** Investigation, Resources. **Malika Abbes:** Data curation, Supervision. **Matteo Gentilucci:** Supervision, Validation. **Tullio Tucciarelli:** Resources, Validation.

Declaration of competing interest

The authors declare that they have no known competing financial interests or personal relationships that could have appeared to influence the work reported in this paper.

Acknowledgements

The authors wish to express their sincere gratitude to the University of Palermo for the financial support of this research. The authors also thank the General Directorate of Water Resources (DGRE) and the Regional Commission for Agricultural Development of Sidi Bouzid (CRDA) for providing the hydrogeological data used in this study. The authors are grateful to all those who contributed, directly or indirectly, to the completion of this work.

Data availability

The authors do not have permission to share data.

References

Anderson, M.P., Woessner, W.W., Hunt, R.J., 2015. Applied Groundwater Modeling: Simulation of Flow and Advective Transport. Academic press.

Ayadi, Y., Gentilucci, M., Ncibi, K., Hadji, R., Hamed, Y., 2025. Assessment of a groundwater potential zone using geospatial artificial intelligence (Geo-AI), remote sensing (RS), and GIS tools in majerda transboundary Basin (North Africa). Water 17 (3), 331. https://doi.org/10.3390/w17030331.

Aydi, W., Saidi, S., Chalbaoui, M., Chaibi, S., Ben Dhia, H., 2013. Evaluation of the groundwater vulnerability to pollution using an intrinsic and a specific method in a GIS environment: application to the Plain of Sidi Bouzid (Central Tunisia). Arabian J. Sci. Eng. 38 (7), 1815–1831. https://doi.org/10.1007/s13369-012-0417-9.

Ben Saad, E., Ben Alaya, M., Taupin, J.D., Patris, N., Chaabane, N., Souissi, R., 2023. A hydrogeological conceptual model refines the behavior of a Mediterranean coastal aquifer system: a key to sustainable groundwater management (Grombalia, NE Tunisia). Hydrology 10 (9), 180. https://doi.org/10.3390/hydrology10090180.

BougHariou, E., Allouche, N., Jmal, I., Mokadem, N., Ayed, B., Hajji, S., et al., 2018. Modeling aquifer behaviour under climate change and high consumption: case study of the Sfax region, southeast Tunisia. J. Afr. Earth Sci. 141, 118–129. https://doi.org/10.1016/j.jafrearsci.2018.02.006.

Castany, G., 1968. Prospection Et Exploitation Des Eaux Souterraines. Dunod, Paris, p. 718.

Castany, G., 1982. Principes et méthodes de l'hydrogéologie. Université De Pierre Et Marie Crue (Paris VI), p. 233p.

Chaabane, C., Zidi, M., Ali, H.H., Touir, J., 2024. The Late Cretaceous polygenic breccias succession of Rouana formation in central Tunisia: implication for the comparison of stratigraphy and depositional environment. Carbonates Evaporites 39 (2), 12. https://doi.org/10.1007/s13146-024-00920-1.

Cid-Escobar, D., Folch, A., Ferrer, N., Katuva, J., Sanchez-Vila, X., 2024. An assessment tool to improve rural groundwater access: integrating hydrogeological modelling with socio-technical factors. Sci. Total Environ. 912, 168864. https://doi.org/10.1016/j.scitotenv.2023.168864.

CRDA (Regional Commission for Agricultural Development of Sidi Bouzid), 2020. Piezometric Records 1990–2020. Internal Report.

DGRE (General Directorate of Water Resources), 2020. Yearbook of Phreatic Aquifer Exploitation, Tunis, Tunisia.

Gharbi, A., Ibn Ali, Z., Abidi, M., Kammoun, A., 2023. Conceptual and numerical hydrogeological modeling of the shallow aquifer of Sidi. In: Selected Studies in Environmental Geosciences and Hydrogeosciences: Proceedings of the 3rd Conference of the Arabian Journal of Geosciences (CAJG-3). Springer Nature, p. 217.

Hajji, S., Karoui, S., Nasri, G., Allouche, N., Bouri, S., 2021. EFA-CFA integrated approach for groundwater resources sustainability in agricultural areas under data scarcity challenge: case study of the Souassi aquifer, central-eastern Tunisia. Environ. Dev. Sustain. 23 (8), 12024–12043. https://doi.org/10.1007/s10668-020-01155-5.

Hamdi, M., Goïta, K., Jerbi, H., Zagrarni, M.F., 2020. Modeling of the natural groundwater recharge under climate change: sisseb El Alem Nadhour Saouaf basin (Central Tunisia) case study. Environ. Earth Sci. 79 (12), 285. https://doi.org/10.1007/s12665-020-09010-6.

Hamed, Y., Ayadi, Y., Khalil, R., Al-Omran, A., Lebdi, F., Dhaouadi, L., 2024a. Wastewater resources, agricultural practices management strategies, soil salinity predictions and artificial recharge in the middle east-Saudi Arabia: a review. J Saudi Society of Agricultural Sci. https://doi.org/10.1016/j.jssas.2024.08.003.

Hamed, Y., Hadji, R., Ahmadi, R., Ayadi, Y., Shuhab, K., Pulido-Bosch, A., 2024b. Hydrogeological investigation of karst aquifers using an integrated geomorphological, geochemical, GIS, and remote sensing techniques (Southern Mediterranean Basin Tunisia). Environ. Dev. Sustain. 26 (3), 6943–6975. https://doi.org/10.1007/s10668-023-02994-8.

Hamed, Y., Hadji, R., Ncibi, K., Hamad, A., Ben Sâad, A., Melki, A., et al., 2022. Modelling of potential groundwater artificial recharge in the transboundary Algero-Tunisian Basin (Tebessa-Gafsa): the application of stable isotopes and hydroinformatics tools. Irrig. Drain. 71 (1), 137–156. https://doi.org/10.1002/ird.2647.

Hamed, Y., Hadji, R., Redhaounia, B., Zighmi, K., Bâali, F., El Gayar, A., 2018. Climate impact on surface and groundwater in North Africa: a global synthesis of findings and recommendations. Euro-Mediterranean Journal for Environmental Integration 3 (1), 25. https://doi.org/10.1007/s41207-018-0067-8.

Izady, A., Davary, K., Alizadeh, A., Ziaei, A.N., Akhavan, S., Alipoor, A., et al., 2015. Groundwater conceptualization and modeling using distributed SWAT-based recharge for the semi-arid agricultural Neishaboor plain, Iran. Hydrogeol. J. 23 (1), 47–68. https://doi.org/10.1007/s10040-014-1219-9.

Jafari, T., Kiem, A.S., Javadi, S., Nakamura, T., Nishida, K., 2021. Fully integrated numerical simulation of surface water-groundwater interactions using SWAT-MODFLOW with an improved calibration tool. J. Hydrol.: Reg. Stud. 35, 100822. https://doi.org/10.1016/j.ejrh.2021.100822.

Jellalia, D., Lachaal, F., Andoulsi, M., Zouaghi, T., Hamdi, M., Bedir, M., 2015. Hydrogeophysical and geochemical investigation of shallow and deep Neogene aquifer systems in Hajeb Layoun-Jilma-Ouled Asker area, Central Tunisia. J. African Earth Sci. 110, 227–244. https://doi.org/10.1016/j.jafrearsci.2015.06.016.

Jmal, I., Ayed, B., Bahloul, M., Boughariou, E., Bouri, S., 2022. Contribution of GIS tools and statistical approaches to optimize the DRASTIC model for groundwater vulnerability assessment in arid and semi-arid regions: the case of Sidi Bouzid shallow aquifer. Arabian J. Geosci. 15 (10), 974. https://doi.org/10.1007/s12517-022-10149-8.

Kauark Leite, L.A., Nascimento, D.O.N., 1993. Développement, Utilisation et Incertitudes des Modèles Conceptuels en Hydrologie. Séminaires Eaux - Environnement N°3 : "Modélisation Du Comportement Des Polluants Dans Les Hydrosystèmes. Paris, (France).

Lachaal, F., Mlayah, A., Bédir, M., Tarhouni, J., Leduc, C., 2012. Groundwater flow modelling in semi-arid regions: the Zéramdine-Béni Hassen Miocene aquifer system (east–central Tunisia), 48, 187-198. https://doi.org/10.1016/j.cageo.2012.05.007.

Langevin, C.D., Hughes, J.D., Banta, E.R., Niswonger, R.G., Panday, S., Provost, A.M., 2017. Documentation for the MODFLOW 6 groundwater flow model (No. 6-A55). US Geological Survey. https://doi.org/10.3133/tm6A55.

Leone, G., Ginolfi, M., Esposito, L., Fiorillo, F., 2024. Relationships between River and Groundwater Flow in an alluvial plain by time series analysis and numerical modeling. Water Resour. Manag. 38 (8), 2851–2868. https://doi.org/10.1007/s11269-024-03795-y.

Liang, F., Li, S., Jie, F., Ge, Y., Liu, N., Jia, G., 2023. The development of a coupled soil water assessment tool-MODFLOW model for studying the impact of irrigation on a regional water cycle. Water 15 (20), 3542. https://doi.org/10.3390/w15203542.

McDonald, M.G., Harbaugh, A.W., 1988. A modular three-dimensional finite-difference ground-water flow model. US Geological Survey Techniques of Water-Resources Investigations. Book 6, Washington, USA (Chapter A1).

Missaoui, R., Abdelkarim, B., Ncibi, K., Gentilucci, M., Brahmi, S., Ayadi, Y., Hamed, Y., 2023. Mapping groundwater recharge potential zones in arid region using remote sensing and GIS perspective, central Tunisia. Euro-Mediterranean J Environ Integration 8 (3), 557–571. https://doi.org/10.1007/s41207-023-00384-0.

Missaoui, R., Abdelkarim, B., Ncibi, K., Hamed, Y., Choura, A., Essalami, L., 2022. Assessment of groundwater vulnerability to nitrate contamination using an improved model in the Regueb Basin, Central Tunisia. Water, Air, Soil Pollut. 233 (8), 320. https://doi.org/10.1007/s11270-022-05806-3.

Moriasi, D.N., Arnold, J.G., Van Liew, M.W., Bingner, R.L., Harmel, R.D., Veith, T.L., 2007. Model evaluation guidelines for systematic quantification of accuracy in watershed simulations. Trans. ASABE 50 (3), 885–900. https://doi.org/10.13031/2013.23153.

Ncibi, K., 2022. Hydrogeological Study and Modeling of Interactions Between Water Reservoirs Under Climatic and Anthropogenic Constraints: a Multidisciplinary Approach in the Sidi Bouzid Basin. University of Gabes, Dissertation, p. 219.

Ncibi, K., Chaar, H., Hadji, R., Baccari, N., Sebei, A., Khelifi, F., Abbes, M., Hamed, Y., 2020a. A GIS-based statistical model for assessing groundwater susceptibility index in shallow aquifer in Central Tunisia (Sidi Bouzid basin). Arabian J. Geosci. 13 (98), 1–21. https://doi.org/10.1007/s12517-020-5112-7.

Ncibi, K., Hadji, R., Hajji, S., Besser, H., Hajlaoui, H., Hamad, A., et al., 2021. Spatial variation of groundwater vulnerability to nitrate pollution under excessive fertilization using index overlay method in central Tunisia (Sidi Bouzid basin). Irrig. Drain. 70 (5), 1209–1226. https://doi.org/10.1002/ird.2599.

Ncibi, K., Hadji, R., Hamdi, M., Mokadem, N., Abbes, M., Khelifi, F., Zighmi, K., Hamed, Y., 2020b. Analytic Hierarchy process and hydrochemical characteristics for roundwater quality assessment of the North-Eastern basin in the Sidi Bouzid region, central Tunisia. Euro-Mediterranean J Environ Integration 5 (1), 19. https://doi.org/10.1007/s41207-020-00159-x.

Ncibi, K., Hamed, Y., Hadji, R., Busico, G., Benmarce, K., Missaoui, R., Wederni, K., 2023. Hydrogeochemical characteristics and health risk assessment of potentially toxic elements in groundwater and their relationship with the ecosystem: case study in Tunisia. Environ. Sci. Pollut. Control Ser. 30 (14), 40031–40048. https://doi.org/10.1007/s11356-022-25016-y.

Saccò, M., Mammola, S., Altermatt, F., Alther, R., Bolpagni, R., Brancelj, A., et al., 2024. Groundwater is a hidden global keystone ecosystem. Glob. Change Biol. 30 (1), e17066. https://doi.org/10.1111/gcb.17066.

Sherwood Lollar, B., Warr, O., Higgins, P.M., 2024. The hidden hydrogeosphere: the contribution of deep groundwater to the planetary water cycle. Annu. Rev. Earth Planet Sci. 52 (1), 443–466. https://doi.org/10.1146/annurev-earth-040722-102252.

Singh, K.G., Pathania, T., 2025. Development and real field application of meshless generalized finite difference method for unconfined groundwater flow modelling. Math. Comput. Simulat. https://doi.org/10.1016/j.matcom.2025.07.027.

Toscani, L., Stefania, G.A., Masut, E., Prieto, M., Legnani, A., Gigliuto, A., et al., 2022. Groundwater flow numerical model to evaluate the water mass balance and flow patterns in Groundwater Circulation wells (GCW) with varying aquifer parameters. Acque Sotterranee 11 (4), 9. https://doi.org/10.7343/as-2022-515.

Trabelsi, F., Tarhouni, J., Mammou, A.B., Ranieri, G., 2013. GIS-based subsurface databases and 3-D geological modeling as a tool for the set up of hydrogeological framework: Nabeul–Hammamet coastal aquifer case study (Northeast Tunisia). Environ. Earth Sci. 70 (5), 2087–2105. https://doi.org/10.1007/s12665-011-1416-y.

Vats, O.P., Sharma, B., Stamm, J., Bhattacharjya, R.K., 2020. Groundwater circulation well for controlling saltwater intrusion in coastal aquifers: numerical study with experimental validation. Water Resour. Manag. 34 (11), 3551–3563. https://doi.org/10.1007/s11269-020-02635-z.

Vellando, P., Juncosa, R., Padilla, F., García-Rábade, H., 2020. Numerical evaluation of groundwater flows: modflow vs. fe models. J. Porous Media 23 (6), 545–562. https://doi.org/10.1615/JPORMEDIA.2020033043.

Zeydalinejad, N., 2022. Artificial neural networks vis-à-vis MODFLOW in the simulation of groundwater: a review. Model. Earth Syst. Environ. 8 (3), 2911–2932. https://doi.org/10.1007/s40808-022-01365-y.